Article

Ultrasensitive Label- and PCR-free Genome Detection based on Cooperative Hybridization of Silicon Nanowires Optical Biosensors

Antonio Alessio Leonardi, Maria josè Lo Faro, Salvatore Petralia, Barbara Fazio, Paolo Musumeci, Sabrina Conoci, Alessia Irrera, and Francesco Priolo

ACS Sens., **Just Accepted Manuscript** • DOI: 10.1021/acssensors.8b00422 • Publication Date (Web): 22 Aug 2018

Ultrasensitive Label- and PCR-free Genome Detection based on Cooperative Hybridization of Silicon Nanowires Optical Biosensors

Antonio Alessio Leonardi[1,2,3,4, †], Maria Josè Lo Faro[4,2, †], Salvatore Petralia[5†], Barbara Fazio[1], Paolo Musumeci[2], Sabrina Conoci[5*], Alessia Irrera[1*], Francesco Priolo[2,4,6*]

1. *CNR-IPCF, Istituto per i Processi Chimico-Fisici, V.le F. Stagno D'Alcontres 37, 98158 Messina, Italy;*

2. Dipartimento di Fisica ed Astronomia, Università di Catania, Via Santa Sofia 64, 95123 Catania, Italy;

3. INFN sezione di Catania, Via Santa Sofia 64, 95123 Catania, Italy;

4. MATIS CNR-IMM, Istituto per la Microelettronica e Microsistemi, Via Santa Sofia 64, 95123 Catania, Italy;

5. STMicroelectronics, Stradale Primosole 50, 95121 Catania Italy;

6. Scuola Superiore di Catania, Via Valdisavoia 9, 95123 Catania, Italy;

* Corresponding Authors: irrera@me.cnr.it, sabrina.conoci@st.com, francesco.priolo@ct.infn.it
† These authors contributed equally to this work

Abstract

The realization of an innovative *label*- and *PCR-free* silicon nanowires (NWs) optical biosensor for direct genome detection is demonstrated. The system is based on the cooperative hybridization to selectively capture DNA and on the optical emission of quantum confined carriers in Si NWs whose quenching is used as detection mechanism. The Si NWs platform was tested with Hepatitis B virus (HBV) complete genome and it was able to reach a Limit of Detection (LoD) of 2 copies/reaction for the synthetic genome and 20 copies/reaction for the genome extracted from human blood. These results are even better than those obtained with the gold standard real time PCR method in the genome analysis. The Si NWs sensor showed high sensitivity and specificity, easy detection method and low

manufacturing cost fully compatible with standard silicon process technology. All these points are key factors for the future development a new class of genetic point of care devices reliable, fast, low cost, easy to use for self-testing including the developing countries.

Keywords: Biosensor, Nanowires, PCR-free, DNA cooperative hybridization, Silicon, Photoluminescence, Hepatitis B virus

Since its discovery in the early 80s, the Polymerase Chain reaction (PCR) has revolutionized the field of genome diagnostics. In fact, ten years later its technological progress led to the invention of *real-time* PCR[1,2] allowing a sensitive and quantitative detection of DNA target sequences in a totally closed-system, minimizing the risk of cross-contamination issues thanks to the use of fluorescence as transduction method[3,4]. For these reasons, PCR is nowadays considered the gold standard method for genome analysis as proven by its large use in a plethora of applications, including determination of viral or bacterial loads in clinical samples, identification and titers of germs in food, diagnosis of tumors, gene expression analysis, or forensic analyses.

However, this methodology is still quite laborious requiring complex instrumentations, qualified personnel and specialized laboratories. These aspects, combined with the high cost of the analysis, limit the PCR capillary pervasion in a large scale for screening and early diagnosis. More severe limitations are present in the developing countries where the infrastructures of clinical laboratory are very poor, and suffer of limited power supply and cost constraints. In these countries, the availability of easy use and low cost methods for genome diagnostic purposes represents a priority task. In fact, this has been identified by the National Institute of Health (NIH) as one of the major priorities in the "Grand Challenges for Global Health"[5]. Therefore, overcoming the limits of the PCR-based methods would open the routes for new perspectives of great impact in the diagnostic field. In this context, the development of new strategies allowing genome detection without any amplification step (*PCR-free* methods) is one of the most challenging research goals that can have a disruptive impact on the reduction of cost, rapidity and bioanalysis complexity[6-8].

Nanostructured silicon photonics is the ideal platform for high sensitivity and selectivity detection of biological molecules in a complex fluidic environment. In this scenario, light emitting Si-based nanostructures are extremely promising materials due to their huge exposed surface and to their optical properties resulting among the most innovative methods of transduction. Indeed, room temperature light emission from quantum confined carriers in nanostructures, such as porous Si (pSi) and Si nanocrystals (NCs), has been already widely explored in literature as an efficient strategy to extract light from this indirect bandgap semiconductor[9-12]. Although appealing, both pSi and NCs are characterized by poor mechanical resistance and high luminescence instability with time. These drawbacks represent severe limitations for pSi and NCs implementation in applicative optical sensing devices. On the contrary, silicon nanowires (NWs) are proven to be featured by relevant physico-chemical properties making them very appealing in several different areas, such as energy[13] photovoltaics [14,15], electronics[16-17], and photonics[18-19].

Concerning the DNA detection, Si NWs have been mainly investigated with electrical transduction method based on the conductance changing upon DNA hybridization with specific probes

immobilized on the NWs surface[20,21]. It has been demonstrated a low limit of detection of 220 attoM (about 6600 DNA target copies per 50 µL) for complementary ssDNA, by using an array of crystalline Si NWs field effect transistor (FET) having diameters below 20 nm[22,23]. The same group showed the possibility to implement up to 24 NWs FET onto a single sensing interface by superlattice nanowire pattern transfer (SNAP) for high throughput and multiplexed biomolecule detection in microfluidic circuit[24]. However, all these DNA electronic sensors require amplification of the DNA target and present the limitations to be cost expensive, time consuming and complex to be integrated in ICs (Integrated Circuits), due to challenges to electronically address individual wires and integrate with conventional manufacturing processes. Moreover, the high background noise of such devices limits their sensitivity. Another very interesting approach is based on the fluorescent labelling of DNA, in particular He's group demonstrated the high sensitivity of Si NWs biochemical sensors for multiplexing detection of different labelled genome sequences pushing the detection limit down to genes[25,26]. In general, labelled detection provides an indirect evidence for the presence of the analyte and could degrade with time and environment exposure, causing also information loss by photobleaching. Other quenching mechanisms can occur also between labels, limiting the detection efficiency.

Biosensors based on the variation of the luminescence properties of NWs upon the adsorption of the target species are recently receiving considerable interest due to their potential performance in sensitivity[27]. However, the luminescence quenching of Si NWs for genomic recognition is still unexplored and detailed studies on the sensing mechanism based on the light emission by NWs upon DNA capture are lacking. Over the years we focused our efforts on the realization of room temperature light emitting Si NWs by metal assisted chemical etching, using thin gold layers[28- 29]. This growth method is based on a low cost process fully compatible with complementary metal-oxide-semiconductor (CMOS) technology and suitable for mass production. By mastering the process parameters, we demonstrated the realization of high-density array of vertical Si NWs with tunable structural properties.

In this paper, we report the first example of direct genome detection without any amplification step (*PCR-free*) and without any label (*Label-free*) in a Si NWs optical biosensor. The proposed strategy employs a chemical approach combining Si NWs with a cooperative *in situ* hybridization of two specific probes, chemically grafted onto the surface, with the genome double strand.

We tested the performances of the sensor using the Hepatitis B virus (HBV) genome. HBV infects today over 3 hundred million people worldwide and it is one of the major causes of liver diseases and liver cancer[30-31]. This addresses the choice of HBV as a designed target for testing our Si NWs optical sensor. The impressive results achieved in sensitivity (2 copies per reactions) are well beyond those

achieved even by PCR and pave the way to future development of a new class of point of care devices, realized at low cost and compatible with Si technology to be used in non-specialized environments.

Experimental

Chemicals and Materials

Commercial n-type doped silicon wafers was purchased by Siegert Wafer. Hydrofluoridric acid (HF) 50%, isopropanol, gold etchant solution, phosphate-buffered saline (PBS) buffer tablets, (3-Glycidyloxypropyl)trimethoxysilane and molecular biology reagent-grade water were purchased by Sigma-Aldrich. The hybridization buffer solution is an aqueous solution of 20mM sodium phosphate buffer (PBS), 1M NaCl (considering NaCl also from PBS tablet), 5.2 mM KCl, 0.1% Tween 20, 2x Denhardt's solution, Salmon sperm DNA 2 μg/ml in molecular reagent-grade water. Hepatitis B virus (HBV) clone complete genome (HBV clone analytical sample) was purchased from Clonit (ref. 05960467) and consists in the entire genome 3.2 kbps and a plasmid PBR322 vector 3.8 kbps provided in a TE (Tris 10 mM,EDTA 1 mM, pH = 8) solution. Micobacterium Tubercolosis (MTB) clone complete genome was obtained from Clonit (ref. 05960564) provided in a TE (Tris 10 mM, EDTA 1 mM, pH = 8) solution.

Analytical HBV genome samples (2, 20, 200, 2000, 200000 copies/reaction) were prepared by diluting the starting clone solution (10^6 copies) in deionised water. HBV genome extraction from human blood (extracted real HBV genome sample) was carried out using Qiagen QIAamp DNA Mini Kit (Ref. 51306), following the Instructions for Use. The experiments were realized in compliance with the Guideline MM13-A: Collection, Transport, Preparation, and Storage of Specimens for Molecular Methods, by Clinical and Laboratory Standards Institute (CLSI), recognized as consensus guideline by the U.S. Food and Drug Administration (FDA). The extraction processes were executed in laboratories certified ISO 9001 and ISO 13485. The mock sample (mock HBV sample) were prepared by spiking different amount of HBV clone (20, 200, 2000 cps/reaction) in serum sample. Extracted real HBV genome samples (20, 200, 2000 copies/reaction) were prepared by diluting the starting solution (10^6 copies) in deionised water.

Silicon Nanowires Synthesis

Silicon NWs are grown by Metal Assisted Chemical Etching (MACE)[32]. Commercially available silicon wafers were first oxidized by UV ozone treatment for 2 min and then immersed in a 5% hydrofluoric acid watery solution for 5 min in order to obtain an oxide-free surface. Subsequently, a thin discontinuous gold layer of 2 nm was deposited onto the oxide-free silicon surface by electron

beam evaporation (EBE) (Kenosistec apparatus) performed at room temperature in an ultra-high vacuum chamber ($<1 \cdot 10^{-8}$ mbar). After the EBE deposition, the samples present nanometric areas of silicon not covered by gold. When the deposited samples are immersed in an aqueous solution of hydrofluoric acid HF (5 M) and hydrogen peroxide H_2O_2 (0.44 M) the gold acts as catalyst promoting the local oxidization only underneath the metal covered regions. The newly formed Si oxide is selectively etched by the HF causing the sinking of the metal mesh into the wafer and the subsequent formation of Si NWs in the remaining uncovered Si regions. Each step of the process is performed at room temperature preventing the diffusion of the gold catalyst into the nanostructures. Finally, the gold layer is removed by using a selective gold etchant solution for 1 min. Unlike other processes, such as vapour-liquid-solid (VLS) approach, this optimized MACE allows for the realization of quantum confined Si NWs[29]. Moreover, it is a low cost, fast and industrially compatible approach that allow to process large area wafers with high throughput and a fine control over the doping and structural properties (radius, length, density) of these Si NWs.

Si NWs Functionalization Protocol

The as-grown Si NWs were treated with by a three process step: (1) cleaning step, (2) vapor phase silanization process and (3) probe anchoring steps.

1) the samples were firstly cleaned for 2 min in an isopropanol bath, rinsed in water for other 2 min, then exposed to UV ozone treatment for 5 min and finally washed in water (2 min) and dried by nitrogen flow at room temperature. This cleaning procedure guarantees the removal of any biological contamination from the Si NWs promoting the uniform formation of an external layer of silicon oxide. Indeed, the SiO_2 layer improves the hydrophilicity of the NWs surface which is an advantage for the functionalization[27].

2) the cleaned surface samples were chemically modified by (3-Glycidyloxypropyl)trimethoxysilane (GOPS) layer. At this scope, the samples were exposed to a 10 ml of GOPS at 120 °C for 4 hours in a low vacuum chamber (200 mbar).

3) after cooling at room temperature the silanized samples were immersed for 4 hours in the aqueous probe solution, (each probe P1 and P2 with a concentration value of 20 μM), in phosphate buffer 150 mM at pH 9.2, at temperature of 30 ±1 °C[33]. After that, the samples were washed three times with molecular biology reagent-grade water in order to remove all the unbound probes and dried by nitrogen flow. The samples were stored at room temperature until the use.

HBV Genome Hybridization

We used a volume of 100 μL of HBV solution applied onto the reaction area of 3x3 mm^2 of the P1/P2-modified-NWs sensor. First of all, we performed the HBV genome denaturation by heating the sample for 4 min at a temperature of 90 °C with the HBV genome solution containing different genomes copies. The hybridization reaction was performed by heating the samples for 2 hrs at 50 ± 0.1°C. Then the samples were washed three times in molecular biology reagent-grade water and dried with a nitrogen flux. The cross-reactivity of our system assay was investigated by using unspecific target consisting in Mycobacterium tuberculosis clone (MTB complete genome purchased from Clonit (ref. 05960564)) with the same protocol.

Characterization Methods

Morphological and structural characterization of the NWs samples are performed by using a Zeiss Supra 25 field-emission scanning electron microscope. Raman measurements were performed focusing an He laser beam tuned at 633 nm onto the NWs samples through a 50X LWD objective (NA = 0.5) and a 100 objective (NA = 0.9) with powers of about 1.5 mW measured on the sample surface. Attenuated Total Reflectance Infrared (ATR-IR) spectroscopic analysis was carried out on as prepared Si NWs and after each functionalization step. IR spectra were acquired in Transmittance mode on a SpectrumTwo PerkinElmer FT-IR spectrometer equipped with a diamond crystal (wavelength range 4000 – 500 cm^{-1}, resolution 2 cm^{-1}, 16 scans). The PL emission by Si NWs after each step is measured using a HR800 Horiba-Jobin Yvon micro-spectrometer in the back-scattering configuration. The PL spectra are acquired using the 364 nm line of an Ar^+ laser, focused on the samples through a 60xUV Olympus objective (NA = 0.9) and used also to collect the emitted light from the samples surface. The PL were performed on the dried sample and the laser spot has a diameter of about 1 μm. For all the measurements the excitation power was maintained fixed at 100 μW measured onto the sample. To verify the confidence of the obtained results we performed ten PL measurements on the same sensor and repeated them for five different Si NWs sensors with the same HBV concentration to attest the repeatability and stability of the results.

Results and discussion

The Si NWs substrate used in this work was prepared according to the previously described method[34], producing an ultra-dense forest of vertically aligned wires (about 10^{12} NWs/cm^2) with length of 3 μm. The scanning electron microscopy (SEM) cross section image of the Si NWs substrate is shown in Figure 1a.

The scheme of the biochemical strategy used for the cooperative hybridization is sketched in Figure 1c-e. More in details, two specific HBV single strand oligonucleotide probes (P1 and P2) were chemically grafted on the Si NWs surface through a treatment with (3-Glycidyloxypropyl) trimethoxysilane (GOPS) producing an epoxy-terminated Si NWs surface able to covalently react with amino-terminated P1 and P2 probes. The surface functionalization with GOPS molecules has been chosen since it is a well known method available in silicon industry which guarantees a stable functionalization[35]. The two P1 and P2 probes anchored to the Si NWs surface are then able to cooperatively hybridize the two complementary HBV genome strands, according to the sketch depicted in Figure 1d. The final system consists in a Si NWs optical sensor whose genome capture ability is based on cooperative hybridization and whose sensing mechanism is based on the photoluminescence (PL) quenching of Si NWs upon the molecular genome recognition (Figure 1e). In order to investigate the performance of the Si NWs sensor, our study started with the test of analytical samples consisting in HBV clone (7144bps) in a concentration range typically used for the calibration curve in the quantitative real time -PCR analyses (2, 20, 200, 2000, 10^5 copies/reaction). To confirm the effectiveness of the cooperative hybridization as an appropriate capture mechanism, we first tested the actual presence of the specific HBV genome by Raman measurements. Figure 2a shows the Raman spectra of as prepared Si nanowires (green line), the same NWs sample after the functionalization procedure with P1 and P2 probes (Si NWs sensor, red line) and after HBV adsorption protocol (Si NWs sensor with HBV, blue line), in the spectral range of interest for genomic recognition. The spectroscopic study performed step by step well attests the success of the functionalization protocol and the presence of HBV in the Si NWs sensor. In particular, the characteristic features associated with amide-I band (1560-1600 cm^{-1}), amide III band (1200-1300 cm^{-1}) of HBV genome[36] and the strong double peak at 1440 cm^{-1} and 1460 cm^{-1} due to the C-H deformation typical of biomolecules are distinguishable from the spectrum of Si NWs sensor with HBV. We also compared this vibrational pattern of the NWs sensor with HBV (blue line) to the Raman spectrum of the same DNA drop casted on a Si substrate and then dried (procedure repeated 5 times on the same point) shown as black line in Figure 2a. It is worthy to note that we can recognize the same spectroscopic contributions, although the better-defined Raman signal coming from HBV in NWs sensor (blue line in Figure 2b) is affected by small shifts and different relative intensities ratio of the Raman bands which lead to a more evident convolution of the spectroscopic features compared to those revealed in Figure 2a. This is due to the different conformations of HBV copies in the two samples: a less chaotic one assumed when HBV is captured by the Si NWs sensor with respect to those assumed by the same genome when it is drop casted several times on Si substrate, on which it forms a sandwich layer.

To further support the conclusion of the Raman characterization on the DNA capture from our Si NWs sensors we have performed Attenuated Total Reflectance IR (ATR-IR) spectroscopy.

IR spectra relevant to as prepared Si NWs (green curve) and functionalized NWs after GOPS silanization (magenta line), Si NWs sensor (red line), Si NWs sensor with HBV (blue line) are shown in Fig. 2c,d,e,f respectively. As prepared Si NWs present a surface oxide layer, as demonstrated by the bands identified at ≈ 1070 cm^{-1} with a small shoulder at ≈ 1200 cm^{-1}. These two represent the Si-O asymmetric stretch (AS) modes. As expected, the silanization process led to a remarkable decrease in ATR-IR% of asymmetric Si-O stretching modes (magenta line). Moreover, weak bands relevant to asymmetric and symmetric C-H stretching at ≈ 2945 and 2875 cm^{-1} can be identified and attributed to alkyl chain of GOPS. In the NWs sensor (figure 2e), the anchoring of DNA probes occurs and can be visualized in the IR spectrum (red curve) in terms of the decrease in ATR-IR% of C-H stretching modes and their slight shift to lower wavenumbers as for the formation of a more packed layer. Additionally, the presence of O-H stretching at ≈ 3390 cm^{-1} is indicative of a certain hydration of single stranded DNA. ATR-IR analysis confirmed the successful hybridization of DNA probes in figure 2f for NWs sensor tested with HBV. In fact, the intense bands between 1740 and 1650 cm^{-1} can be undoubtedly ascribed to C=O, C=N stretching, and exocyclic $–NH_2$ bending vibrations of the DNA bases (orange asterisk). Moreover, purine ring mode was identified at 1460 cm^{-1} (brown asterisk). Unfortunately, the characteristic signals such as the stretching modes of PO_2 group related to the DNA phosphodiester backbone (1080, 1230 cm^{-1}) could not be discriminated due to the Si-O stretching bands. However, the slight shift to lower wavenumber and the significant decrease in ATR-IR% of O-H stretching band indicates the capture of HBV DNA in figure 2f.

Once demonstrated the capture of HBV DNA, we tested the sensors by measuring the variations in optical emission as a function of copies/reaction. Figure 3a shows a comparison of the room temperature photoluminescence (PL) spectra of the Si NWs sensors tested in a buffer solution reported for different numbers of HBV clone copies/reaction (cps) ranging from 2 to 10^5 cps. The spectra are characterized by a broad PL band peaked at 700 nm, which is the typical emission of the Si NWs under the excitation at 364 nm with a laser power of about 100 μW due to the quantum confinement effect[37]. All the PL spectra were obtained at room temperature and are the average of ten PL spectra in different points of the same sensor achieving the same experimental results within the considered errors. To verify the correctness of the obtained results we performed analogue PL measurements on five Si NWs sensors, attesting the repeatability of the results. The black spectrum is the signal of the sensor (with probe P1 and P2) immersed in a buffer solution without any copy of HBV and it represents our reference signal. The decrease of the PL signal is clearly visible by increasing the number of the HBV cps from 2 to 2000. It is evident that already at 2 cps the signal

shows a clear quenching. Above 2000 copies/reaction and up to 10^5 cps the sensor does not show any more a clearly distinguishable PL variation and so it reaches a saturation state. The interaction between the HBV and the functionalized NWs determines the quenching of the PL signal used as detection mechanism.

The effect of a biological matrix and its possible interferences can be assessed by testing the Si NWs sensor with HBV clone genome dissolved in human serum (Figure 3b) instead of the buffer solution. These spectra are characterized by two multi-peaked bands at 700 nm, due to the Si NWs emission[29] and in the range 400-600 nm, respectively. By comparing the PL spectra of these Si NWs sensor in the case of the testing in buffer solutions (Figure 3a) with those in human serum solution (Figure 3b), it is reasonable to attribute the emission of the broad multi peaked band at 400-600 nm to the human serum matrix effect. To confirm this hypothesis, a Si wafer (without NWs) was tested with a solution composed by human serum without HBV and the same broad multi peaked band 400-600 nm was observed (data not showed).

Figure 3c reports as blue dots an analysis of the experimental data, i.e. the PL intensities variation of the Si NWs sensor tested in a buffer solution as a function of the HBV copies (Figure 3a), integrated from 550 to 850 nm and normalized to the reference signal in buffer. The red dashed region is for these points the PL signal of the sensor tested in the buffer solution without HBV and it represents therefore the reference sensor signal. From the data reported in Figure 3c, the Si NWs sensor shows a limit of detection (LoD) of 2 HBV cps in buffer detectable without any kind of amplification of the pathogen genome. In fact, the difference of the 2 copies from the reference is of about 19% and hence clearly distinguishable. By increasing the number of HBV copies/reaction by one order of magnitude, a relative PL reduction by a further 20% is noted. Above 2000 cps and up to 10^5 cps a PL variation of only 4% attests that the saturation trend is reached. It is remarkable that the obtained LoD of 2 copies per reaction is even lower than that declared by quantitative real time PCR corresponding to 10 copies/reaction[38-39].

In Figure 3c, as orange dots, the integrated PL signals of the NWs sensors tested with HBV dissolved in human serum are reported as a function of the number of HBV clone cps. The PL are normalized to the reference signal obtained in a serum matrix without HBV represented by the red dashed region. The PL integrated signals were calculated by de-convolving the NWs peaks in Figure 3b subtracting the part of the signal coming from serum and considering the Gaussian area ascribed only to the NWs PL emission at around 700 nm (integrated between 550 and 850 nm). The integrated signal obtained by the reference in human serum is a 1.23 factor lower than the signal obtained in buffer. In order to compare the two trends in different fluid matrices the dash red bar in figure 3c is the reference signal

of the sensor obtained in their respective matrix (buffer or human serum) without any copy of DNA plotted to the same value of 1.

This graph clearly attest that the PL signal variation of the NWs sensor as a function of HBV concentration is the same in the two matrices. In fact, as is possible to observe, the orange (test in serum) and blue (test in buffer) dots overlap at the same values. Thus, the PL quenching percentage is identical when the same genome is detected, independently of the fluid matrix.

This is a demonstration of the selectivity which is crucial for a real medical sensor and of the capability of the sensor to correctly operate in a complex real matrix.

A crucial point for a real use in the medical field is the selectivity. To address this point, the Si NWs sensor was hence tested in presence of 2000 cps of unspecific genome consisting in Mycobacterium Tuberculosis (MTB) both in buffer (green square) and human serum (violet triangle), as shown in Figure 3c. The PL signal of 2000 MTB cps measured in buffer and in human serum is about the same of their respective reference signals of the sensors, confirming that no hybridization occurred. This experimental evidence proves that the Si NWs sensor is highly selective for HBV demonstrating huge potentiality for applications.

For real medical use, the performance assessment of the Si NWs sensor with real samples is a crucial point to be addressed. To further investigate this point, we tested the device by using a real HBV genome extracted from a blood sample. The sample was selected to assess the effectiveness of our sensor towards the real HBV genome that differs from the synthetic clone in the length: 7144 bps for HBV clone *versus* 3300 bps for real genome. Figure 4 reports the results obtained for an extracted HBV real sample tested in buffer. The black curve in Fig. 4a is the PL spectrum of the sensor in the buffer without any HBV copy (reference signal of the sensor with P1 and P2). By increasing the HBV copies/reaction number from 20 cps to 2000 cps, a decrease of the PL signals is observed, clearly distinguishable from the reference already from 20 copies/reaction. This value can be considered the LoD of the Si NWs sensor under testing conditions close to the real case. Figure 4b reports the PL intensities of the Si NWs sensor tested with real HBV as a function of the real HBV copies, integrated from 550 to 850 nm and normalized to the reference signal. The reference signal in the buffer is reported as a red dashed region. It is noteworthy that this Si NWs sensor is able to detect the real HBV genome extracted from human blood with an efficiency comparable to the real time PCR (20 cps/reaction), even if its length is about half of the analytical sample.

Conclusions

In this work we describe the direct genome detection without any amplification step (*PCR-free*) and without any label (*Label-free*) based on the PL quenching of a Si NWs sensor. The platform, tested with HBV genome, has proven to reach a LoD of 2 copies/reaction for synthetic genome in a buffer solution and 20 copies/reaction for genome in real samples. Particularly relevant is the ability of the Si NWs optical sensor to detect without any label and amplification step the complete genome in a biological matrix at high complexity, like serum, where there is the presence of a huge amount of possible interfering molecules, such as proteins or nucleic acids. The designed strategy based on cooperative hybridization for the DNA capture and on Si NWs quantum confinement luminescence quenching for detection, guarantees both specificity and versatility being considered for general purpose. In fact, by changing the probe type in the functionalization protocol it is possible to realize a sensor for the specific detection of different genomes. The sensitivity, easy detection method and the low manufacturing cost fully compatible with standard silicon process technology permits the development of competitive miniaturised device for genome analysis. All these points are key factors for the future development a new class of genetic point of care devices reliable, fast, low cost, easy to use for self-testing including the developing countries.

Acknowledgments

G. Lupò, D. Arigò, G. Gismondo, R. Caruso, G. Spinella, and C. Percolla are acknowledged for expert technical assistance. PON SISTEMA (MIUR) Project is acknowledged for partial financial support. A.I. acknowledges the Project PON_00214_1 named TECLA.

References

(1) Heid, C. A.; Stevens, J.; Livak, K. J.; Williams, P. M. Real time quantitative PCR. *Genome Res.* **1996**, 6, 986-994.

(2) Mackay, M. I. Real-time PCR in the microbiology laboratory. *Clin. Microbiol. Infect. Dis.* **2004**, 10, 190–212.

(3) Almassian, D. R.; Cockrell, L. M.; Nelson, W. M. Portable nucleic acid thermocyclers. *Chem. Soc. Rev.*, **2013**, 42, 8769−8798.

(4) Nurmi, J.; Wikman, T.; Karp, M.; Lövgren, T. High-Performance Real-Time Quantitative RT-PCR Using Lanthanide Probes and a Dual-Temperature Hybridization Assay. *Anal. Chem.* **2002**, 74, 14, 3525-3532.

(5) Mabey, D.; Peeling, R. W.; Ustianowski, A.; Perkins, M. D. Tropical infectious diseases: Diagnostics for the developing world. *Nat. Rev. Microbiol.* **2004**, 2, 231−240.

(6) Vollmer, F.; Yang, L. A review of microcavity biosensing mechanisms. *Nanophotonics* **2012**, 1, 267–291.

(7) Wang, J. Nanomaterial-based electrochemical biosensors. *Analyst* **2005**, 130, 421–426.

(8) Petralia S.; Conoci, S. PCR Technologies for Point of Care Testing: Progress and Perspectives. *ACS Sens.* **2017**, 2, 876-891.

(9) Zhang, H.; Jia, Z. ; Lv, X.; Zhou, J.; Chen, L.; Liua, R.; Ma, J. Porous silicon optical microcavity biosensor on silicon-on-insulator wafer for sensitive DNA detection. *Biosens. Bioelectron.* **2013**, 44, 89–94.

(10) Chan, S.; Fauchet, P. M. Tunable, narrow, and directional luminescence from porous silicon light emitting devices. *Appl. Phys. Lett.* **1999**, 75, 274-276.

(11) Irrera, A.; Pacifici, D.; Miritello, M.; Franzò, G.; Priolo, F. Excitation and de-excitation properties of silicon quantum dots under electrical pumping. *Appl. Phys. Lett.* **2002**, 81, 1866-1868.

(12) Pavesi, L.; Dal Negro, L.; Mazzoleni, C.; Franzò, G.; Priolo, F. Optical gain in silicon nanocrystals. *Nature* **2000**, 408, 440–444.

(13) Chan, C. K.; Peng, H.; Liu, G.; McIlwrath, K.; Zhang, X. F.; Huggins, R. A.; Cui, Y. High-performance lithium battery anodes using silicon nanowires. *Nat. Nanotechnol.* **2008**, 3, 31-35.

(14) Garnett, E.; Yang, P. Light Trapping in Silicon Nanowire Solar Cells. *Nano Lett.* **2010**, 10, 3 1082–1087.

(15) Tian, B.; Zheng, X.; Kempa, T. J.; Fang, Y.; Yu, N.; Yu, G.; Huang, J.; Lieber, C. M. Coaxial silicon nanowires as solar cells and nanoelectronic power sources. *Nature* **2007**, 449, 885–889.

(16) Heinzig, A.; Slesazeck, S.; Kreupl, F.; Mikolajick, T.; Weber, W. M. Reconfigurable Silicon Nanowire Transistors. *Nano Lett.* **2012**, 12, 1 119−124.

(17) Mirza, M. M.; Schupp, F. J.; Mol, J. A.; MacLaren, D. A.; Briggs, G. A. D. ; Paul, D. J. One dimensional transport in silicon nanowire junction-less field effect transistors. *Sci. Rep.*, **2017**, 3004, 1-7.

(18) Fazio, B.; Irrera, A.; Pirotta, S.; D'Andrea, C.; Del Sorbo, S.; Lo Faro, M. J.; Gucciardi, P. G.; Iatì, M. A.; Saija, R.; Patrini, M.; Musumeci, P.; Vasi, C. S.; Wiersma, D. S.; Galli, M.; Priolo, F. Coherent backscattering of Raman light. *Nat. Photonics* **2017**, 11, 170–176.

(19) Fazio, B.; Artoni, P.; Iatì, M. A.; D'Andrea, C.; Lo Faro, M. J.; Del Sorbo, S.; Pirotta, S.; Gucciardi, P. G.; Musumeci, P.; Vasi, C. S.; Saija, R.; Galli, M.; Priolo, F.; Irrera, A. Strongly enhanced light trapping in a two-dimensional silicon nanowire random fractal array. *Light: Sci, Appl.* **2016**, 5, e16062, 1-7.

(20) Shao, M.-W.; Shan, Y.-Y.; Wong, N.-B.; Lee, S.-T. Silicon Nanowire Sensors for Bioanalytical Applications: Glucose and Hydrogen Peroxide Detection. *Adv. Funct. Mater.* **2005**, 15, 1478-1482

(21) Mukhopadhyay, R.; Lorentzen, M.; Kjems, J; Besenbacher, F. Nanomechanical Sensing of DNA Sequences Using Piezoresistive Cantilevers. *Langmuir* **2005**, 21, 18, 8400-8408.

(22) McAlpine, M. C.; Ahmad, H; Wang, D.; Heat, J. R. Highly ordered nanowire arrays on plastic substrates for ultrasensitive flexible chemical sensors. *Nat. Mater.* **2007**, 6, 379–384.

(23) Cheng, M. M.-C.; Cuda, G.; Bunimovich, Y. L.; Gaspari, M.; Heath, J. R.; Hill, H. D.; Mirkin, C. A.; Nijdam, A. J.; Terracciano, R.; Thundat, T.; Ferrari, M. Nanotechnologies for biomolecular detection and medical diagnostics. *Curr. Opin. Chem. Biol.* **2006**, 10, 11–19.

(24) Beckman, R.; Johnston-Halperin, E.; Luo, Y.; Green, J. E.; Heath, J. R. Bridging dimensions: demultiplexing ultrahigh-density nanowire circuits. *Science* **2005**, 310, 465-468.

(25) Su, S.; Wei, X.; Zhong, Y.; Guo, Y.; Su, Y.; Huang, Q.; Lee, S.-T.; Fan, C.; He, Y. Silicon nanowire-based molecular beacons for high-sensitivity and sequence-specific DNA multiplexed analysis. *ACS Nano* **2012**, 6, 2582–2590.

(26) Xie, J.; Jiang, X.; Zhong, Y.; Lu, Y.; Wang, S.; Wei, X.; Su, Y.; He, Y. Stem-loop DNA-assisted silicon nanowires-based biochemical sensors with ultra-high sensitivity, specificity, and multiplexing capability. *Nanoscale* **2014** 6, 9215–9222.

(27) Irrera, A.; Leonardi, A. A.; Di Franco, C.; Lo Faro, M. J.; Palazzo, G.; D'Andrea, C.; Manoli, K.; Franzò, G.; Musumeci, P.; Fazio, B.; Torsi, L.; Priolo, F. New Generation of Ultrasensitive Label-Free Optical Si Nanowire-Based Biosensors. *ACS photonics* **2018**, 5, 2 471–479.

(28) Lo Faro, M. J.; D'Andrea, C.; Messina, E.; Fazio, B.; Musumeci, P.; Reitano, R.; Franzò, G.; Gucciardi, P. G.; Vasi, C.; Priolo, F.; Iacona, F.; Irrera, A. Silicon nanowire and carbon nanotube hybrid for room temperature multiwavelength light source. *Sci. Rep.* **2015**, 5, 16753, 1-10.

(29) Priolo, F.; Gregorkiewicz, T.; Galli, M.; Krauss T. F. Silicon nanostructures for photonics and photovoltaics. *Nat. Nanotechnol.*, **2014**, 9, 19–32.

(30) Bandhavkar, S. Developing Strategies for Early Detection of Hepatitis B Infection. *Clin. Microbiol.* **2016**, 5, 234, 1-3.

(31) Gitlin, N. Hepatitis B: diagnosis, prevention, and treatment. *Clin. Chem.* **1997**, 43, 8(B) 1500–1506.

(32) D'Andrea, C.; Lo Faro, M. J.; Bertino, G.; Ossi, P. M.; Neri, F.; Trusso, S.; Musumeci, P.; Galli, M.; Cioffi, N.; Irrera, A.; Priolo, F.; Fazio, B. Decoration of silicon nanowires with silver nanoparticles for ultrasensitive surface enhanced Raman scattering. *Nanotechnology* **2016**, 27, 375603, 1-12.

(33) Petralia, S.; Sciuto, E. L.; Di Pietro, M. L.; Zimbone, M.; Grimaldi, M. G.; Conoci, S. Innovative Chemical Strategy for PCR-free Genetic Detection of Pathogens by an Integrated Electrochemical Biosensor. *Analyst* **2017**, 142, 2090–2093.

(34) Irrera, A.; Lo Faro, M. J.; D'Andrea, C.; Leonardi, A. A.; Artoni, P.; Fazio, B.; Picca, R. A.; Cioffi, N.; Trusso, S.; Franzò, G.; Musumeci, P.; Priolo, F.; Iacona, F. Light-emitting silicon nanowires obtained by metal-assisted chemical etching. *Semicond. Sci. Technol.* **2017**, 32, 4, 043004, 1-20.

(35) Petralia, S.; Cosentino, T.; Sinatra, F.; Favetta, M.; Fiorenza, P.; Bongiorno, C.; Sciuto, E. L.; Conoci, S.; Libertino, S. Silicon Nitride Surfaces as Active Substrate for Electrical DNA Biosensors. *Sens. Actuators B: Chem.*, **2017**, 252, 492–502.

(36) Anwar, S.; Firdous, S. Optical diagnostic of hepatitis B (HBV) and C (HCV) from human blood serum using Raman spectroscopy. *Laser Phys. Lett.* **2015**, 12, 076001, 1-5.

(37) Pecora, E. F.; Lawrence, N.; Gregg, P.; Trevino, J.; Artoni, P.; Irrera, A.; Priolo, F.; Dal Negro, L. Nanopatterning of silicon nanowires for enhancing visible photoluminescence. *Nanoscale* **2012**, 4, 2863-2866.

(38) Forootana, A.; Sjöbackc, R.; Björkmanc, J.; Sjögreen, B.; Linz, L.; Kubistace, M. Methods to determine limit of detection and limit of quantification in quantitative real-time PCR (qPCR). *Biomol. Detect. Quantif.*, **2017**, 12, 1-6.

(39) Hoy, M. A. DNA Amplification by the Polymerase Chain Reaction. *Molecular Biology Made Accessible Insect Molecular Genetic (3rd edition)*, **2013**, chapter 8, 307-372.

Figures

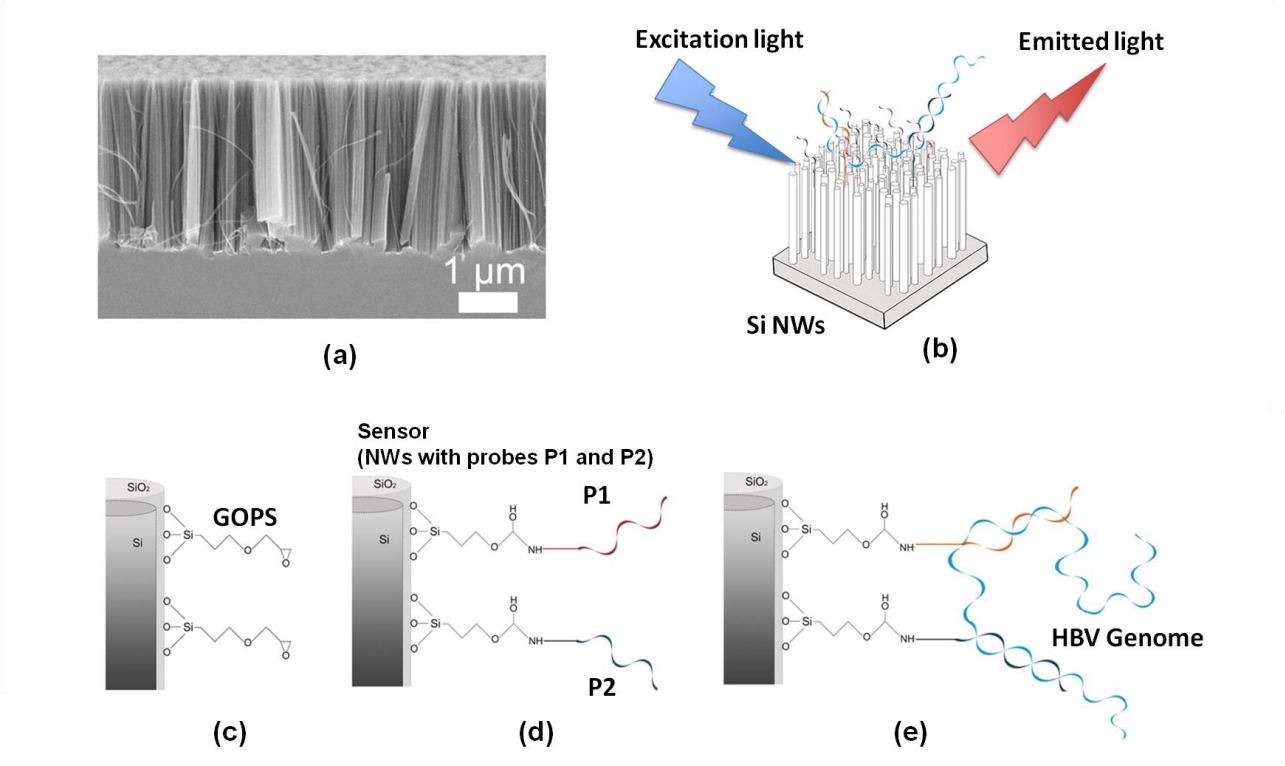

Figure 1: a) Cross section SEM image of a Si NWs vertical array with length of about 3 µm. b) Schematic of the concept of the NWs optical sensor. Schematic illustration of the NWs surface functionalization for HBV cooperative hybridization recognition: c) silanization of the Si NWs surface with GOPS after the cleaning procedure, d) NWs sensor reference obtained after the anchoring of two specific complimentary probes for HBV probes P1 and P2 and e) capture of HBV by the probe P1 and P2 due to cooperative hybridization.

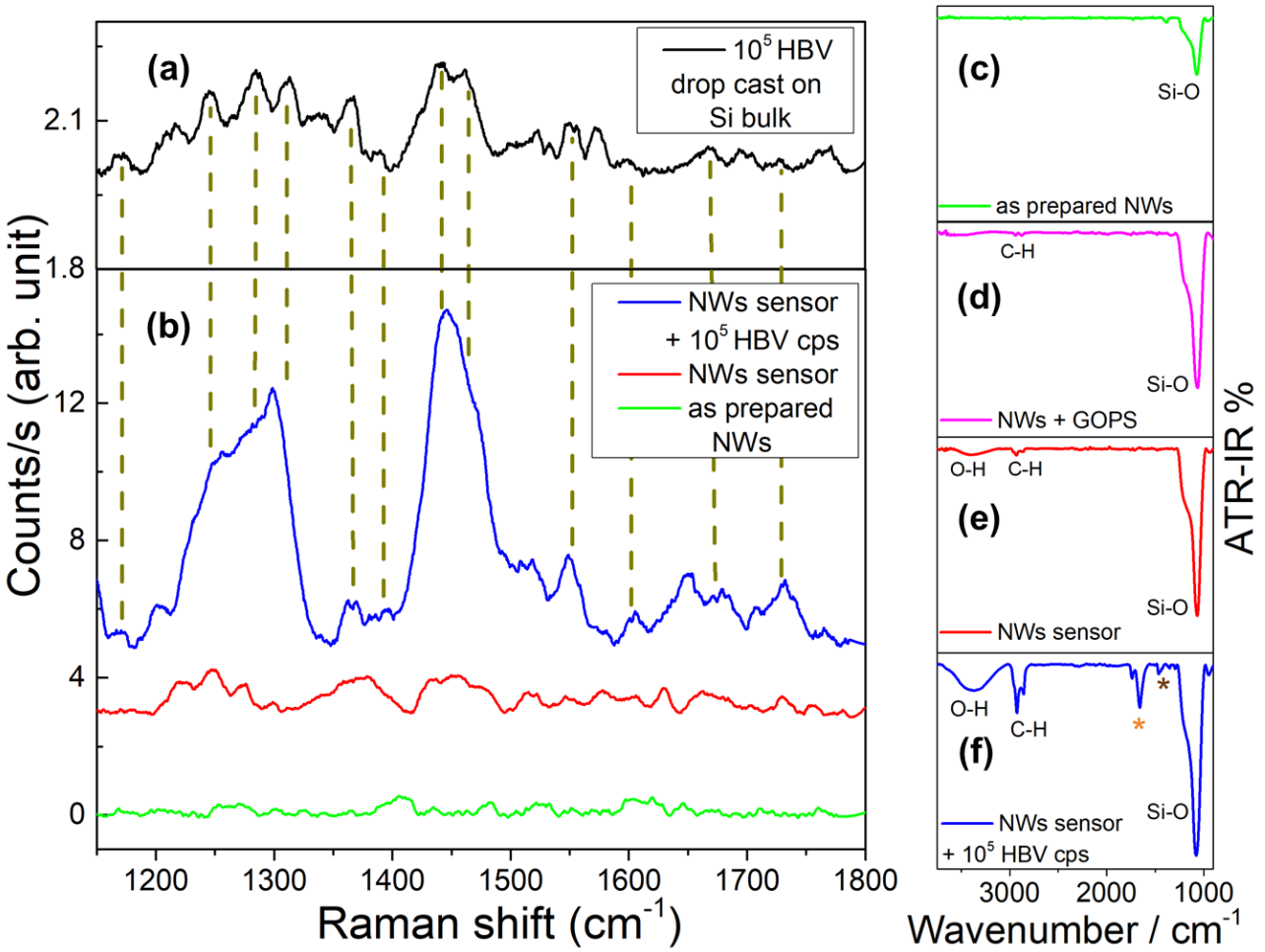

Figure 2: a) The Raman spectrum of 10^5 HBV cps drop casted (5 times on the same point) onto Si bulk wafer without any functionalization is shown in black as a reference for the Raman peak identification of the presence of HBV DNA. b) Raman spectra of as-prepared Si nanowires (green line), NWs sensor after the functionalization procedure (red line) and after the adsorption protocol with 10^5 HBV clone cps tested in buffer (blue line) are shown in the spectral range of interest for HBV recognition. In figure 2 are reported the ATR-IR spectra relevant to c) as prepared Si NWs (green curve) and d) functionalized NWs after GOPS silanization (magenta line), e) Si NWs sensor (red line), f) Si NWs sensor with HBV (blue line).

.

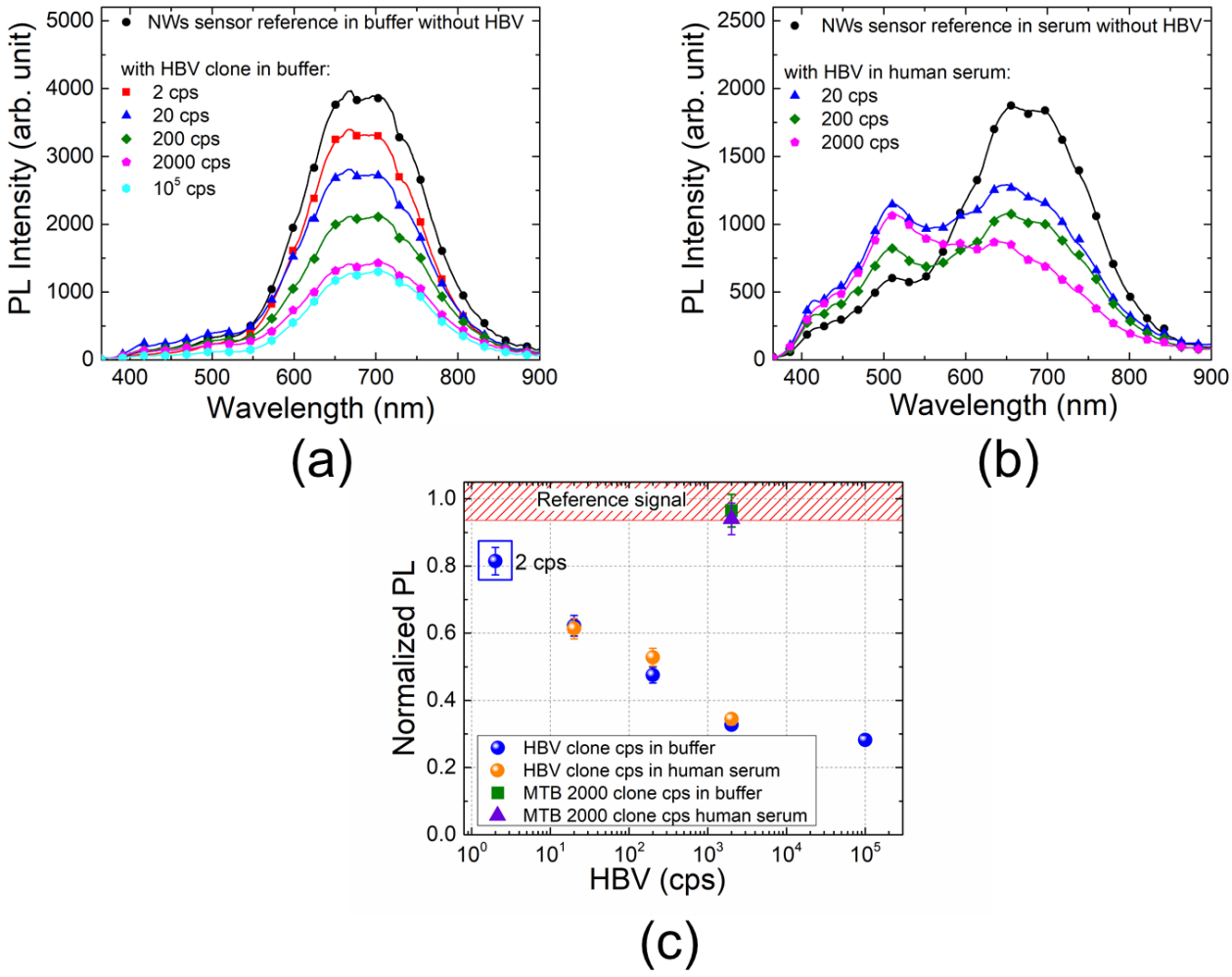

Figure 3: PL spectra of the NWs sensors reported for different HBV clone concentrations tested in buffer solution and human plasma are reported in a) and b), respectively. All PL measurements were performed ten times on the same sensor and repeated them for five different Si NWs sensors with the same HBV concentration to attest the repeatability and stability of the results.
The PL reference spectra of the NWs sensors without any copies of HBV are shown in black for both (a) buffer and (b) human serum solutions. The trend of the PL integrated peaks of the NWs sensors tested as a function of HBV clone concentration in buffer (blue dots) and in serum (orange dots) are shown in figure 3(c). For each HBV concentration, the PL integrated peaks are normalized for each reference signal (red dashed region) of the sensor. The green square shown in figure (c) is the PL integrated peak (normalized to the buffer reference signal) of the NWs sensor tested for 2000 MTB clone cps in buffer, while the violet triangle is the PL integrated peak (normalized to the human serum reference signal) of the NWs sensor tested for 2000 MTB clone cps in human serum.

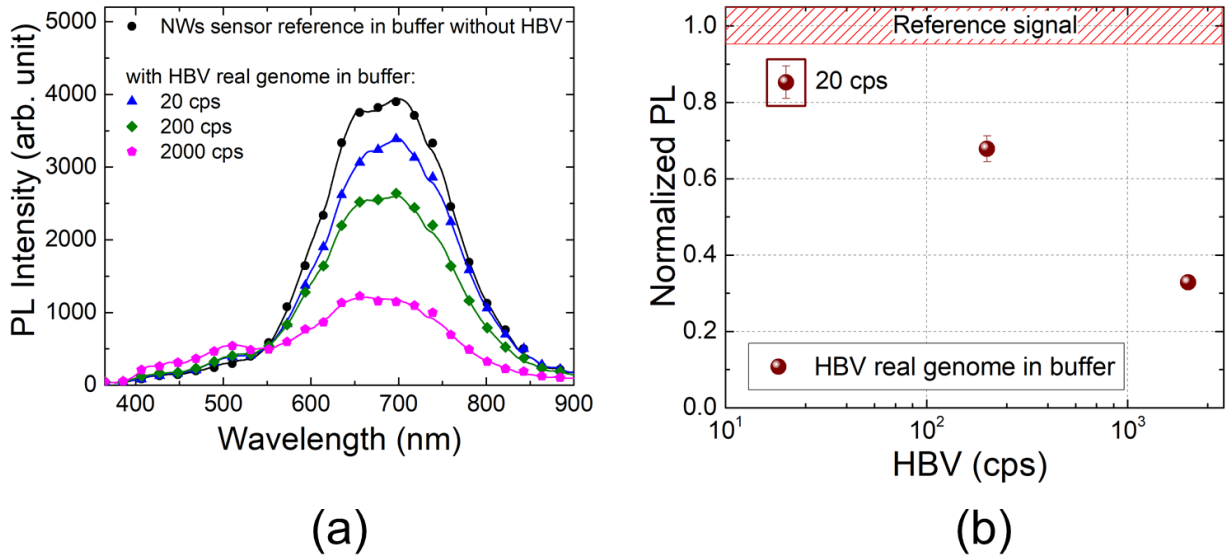

Figure 4: a) PL spectra of the NWs sensor tested in HBV real genome extracted from infected human blood and spiked in buffer reported for different concentrations ranging from 20 cps up to 2000 cps. The PL reference of the sensor without any copies of HBV is shown in black. b) Trend of the PL integrated peak of the de-convolved NWs PL emission as a function of real HBV genome concentration normalized to its reference signal (red bar) obtained by the buffer solution without any real HBV copy.

For TOC only